J2.19

THE AIR QUALITY FOUR-PANEL CHART

William F. Ryan
The Pennsylvania State University, University Park, Pennsylvania

George M. Bridgers
State of North Carolina, Division of Air Quality, State of North Carolina, Raleigh, North Carolina

Daniel D. Salkovitz
Virginia Department of Environmental Quality, Richmond, Virginia

Charles A. Piety
University of Maryland, College Park, Maryland

1. INTRODUCTION

There has been a rapid increase in the number of locations providing air quality forecasts over the past decade. In the early 1990's, only a handful of locations, primarily in California, issued routine air quality forecasts. At the current time, over 300 cities and metropolitan areas issued daily forecasts (www.epa.gov/airnow/) (Figure 1). In addition to providing the basis for public health warnings, air quality forecasts are used for episodic emissions control programs. Many cities, have "Ozone Action Days" where coordinated emissions reduction programs are set into motion based on air quality forecasts. The expanding need for air quality forecasts coupled with improvements in numerical chemical models and computational speed have resulted in the development and deployment of operational numerical air quality prediction models (Mass et al, 2003; McHenry et al., 2003; McHenry et al., 2000). In the summer of 2003, NOAA tested a regional scale air quality forecast model (http://www.nws.noaa.gov/ost/air_quality/index.htm). In anticipation of the widespread use of numerical models to provide air quality forecast guidance, this paper discusses the needs of air quality forecasters with respect to numerical model output. The unique forecast issues posed by air quality require a different set of forecast images than those traditionally provided by synoptic scale meteorological models.

2. THE AIR QUALITY FORECAST PROBLEM

The air quality forecast parameters of current interest are ozone (O_3) and fine particulate matter ($PM_{2.5}$). O_3 and, and a portion of $PM_{2.5}$, are secondary pollutants formed by the interaction of primary emissions, often termed precursors. For example, motor vehicle exhaust contains both hydrocarbons and oxides of nitrogen that combine to form O_3. Both the emissions of precursors and the production rate of secondary pollutants are sensitive to meteorological factors. In order to interpret and analyze air quality model output, forecasters will need to analyze both the air quality model output as well as its underlying meteorological fields. As a result, integrated images from both the meteorology and chemistry models must be provided to the forecasters.

For air quality forecasting, there are a set of unique recurring issues that can serve as the framework for selecting the optimal set of model images. These issues include: (1) Persistence of the forecast parameters; (2) Transport of pollutants on local and regional scales; (3) Depth and evolution of the layer within which the pollutants are mixed; (4) Photo-chemical processes occurring within the mixed layer; (5) Variations in concentrations driven by small-scale processes; and, (6) Timing of the forecasts. Each of these issues and the implications for forecast guidance is addressed below.

Both O_3 and $PM_{2.5}$ have lifetimes on the order of days. As a result, persistence of concentrations is a major factor in any forecast. In the mid-Atlantic, peak O3 concentrations have an auto-correlation of 0.5-0.6 with a lag of one day (Ryan et al., 2000). Persistence is often an accurate 24-hour forecast. The lifetime of the pollutants of interest is sufficiently long that transport of pollutants and precursors on both local and regional scales is important (Dickerson, Doddridge and Rhoads, 1995; Ryan et al., 1998; Knapp et al., 1998). Information on the movement of pollutants and current concentrations is a forecast priority. The sources of pollutant emissions are at or near the surface and the transformation and production of secondary pollutants occur primarily in the well-mixed boundary layer. To the extent that boundary layer

* *Corresponding author address*: William F. Ryan, Pennsylvania State University, Department of Meteorology, 409 Walker Building, University Park, PA, 16802, email: wfr1@psu.edu.

depth is reduced, for example, by warm air advection, concentrations of pollutants will rise. Photochemical processes produce O_3, and a fraction of $PM_{2.5}$. Forecasters need to know the extent of UV radiation reaching the near surface layer. That need, in turn, requires knowledge of cloud cover and optical thickness. Although regional scale concentrations of O_3 and $PM_{2.5}$ set the daily baseline of pollutant concentrations, it is also true that large variation in peak levels occur on the order of 10's of km. Local scale processes, for example, land and sea breeze, are often critical forecast issues. Finally, because a key use of the forecasts is to initiate voluntary pollution control programs, the forecasts must be issued at a long lead-time. Typically, the forecasts are issued at 1600-2000 UTC and are valid the following day.

3. AIR QUALITY FORECAST IMAGES

With the critical forecast issues noted above in mind, a framework containing a subset of key elements that can be utilized in the 4-panel chart is proposed (Figure 2).

The most important panel (top left) will be the air quality forecast itself, valid on the succeeding day. Air quality health standards and, by reference, the air quality forecasts, are based on a peak concentration at any location within a forecast area. For O_3, the maximum 8-hour average is the forecast parameter; while for $PM_{2.5}$ a daily (24 hour) average is the standard. The forecast image must provide a measure of peak concentrations. An example from the NOAA experimental air quality forecast model is provided in Figure 3. While not shown here, additional images related to forecast concentrations should also be available (Table 1). The most important of these are hourly loops and changes in concentration from the previous forecast run. While air quality forecast models cannot reasonably be expected to diagnose peak concentrations on the very fine scale (10's of km) at which they occur in nature, experienced forecasters with knowledge of local emissions patterns, can often deduce the occurrence of extreme local concentrations based on the interplay of plume placement and emissions. A loop, showing the movement and evolution of the high pollutant plume is therefore of great utility. Trends in pollutant forecasts from run to run (lagged-average forecasts, or "*d*(prog)/dt) may also provide useful information to forecasters although this assumption requires corroborative research (Hamill, 2003).

Because air quality forecast models are complex, containing a number of sub-models for emissions, model performance and bias will be significant issues. Experience with numerical air quality models used for pollution reduction strategy development has shown that systematic biases are common. Forecasters will benefit from continually updated model bias information similar to what is currently provided for meteorological models (e.g., http://www.hpc.ncep.noaa.gov/html/model2.shtml). Ideally, this information would be both short term, analyzing performance on the synoptic scale (2-3 days), and longer term (weeks, or seasons) to provide more systematic bias measures. The limitation of this approach is that the forecast model will likely not be "frozen" in any one form for some time.

As noted above, O_3 and $PM_{2.5}$ have relatively long lifetimes, particularly with respect to the 2-5 day synoptic cycle. As a result, knowledge of current air quality conditions, particularly upwind of a forecast area, is critical. Currently, observations of pollutant concentrations, in near real-time, are provided by the EPA (http://www.epa.gov/airnow). For efficient analysis of forecast information, it is imperative that this information be available concurrently with the forecast. The type of observational data presented will also depend on the forecast parameter of interest. O_3 observations have a strong diurnal cycle, with the exception of high elevation sites that remain above the nocturnal boundary layer, which constrains the useful period of observed concentrations (Figure 4). In the nighttime hours, O_3 trapped beneath the nocturnal inversion is destroyed upon deposition to the surface. With no ultra-violet (UV) radiation available to produce more O_3, concentrations near the surface decline rapidly in the overnight hours. Above the nocturnal boundary layer, however, O_3 is approximately conserved. Therefore, surface based monitors fail to observe the overnight "reservoir" of O_3. By late morning, as the surface inversion breaks, O_3 is mixed downward, leading to rapid rises in concentrations reflecting the regional O_3 load (Figure 5). A diagnosis of "true" persistence O_3, can only be made after the surface based inversion breaks, often 1400-1600 UTC. In addition to informing forecasters on persistence issues, observations made ~ 1600 UTC will allow verification of short-range model results. However, numerical O_3 models tend to show poor performance in the overnight hours and some uncertainty related to model initialization ("spin up") may be a factor limiting the utility of this information.

Assuming observed concentrations are available in near real-time, a combination of current concentrations and trajectory model results can provide information on the magnitude of transported pollutants. Trajectory models are currently run independently of the air quality model. An example of standard output from the NOAA-ARL HYSPLIT model, is shown in Figure 6 (Draxler and Rolph, 2003; Rolph, 2003). Ideally, a back trajectory model would be integrated with the meteorological model driving the chemistry model and real-time chemistry data. A mock-up of such an image, using an O_3 forecast from the NOAA forecast model, is provided in Figure 7. There are problems determining regional scale transport of pollutants using back trajectories. First, pollutant concentrations are observed only at the surface. The assumption that surface observations near mid-day reflect a well mixed boundary layer may not always be correct. Chemical transformations will occur along the air parcel path, particularly for $PM_{2.5}$, so that only qualitative conclusions can be reached with respect to concentrations at the point of trajectory termination. It is possible to incorporate chemical transformation calculations into the back trajectory model (Stein et al, 2000). Finally, back trajectories lose accuracy near the surface, where the air quality monitors are located, due to vertical wind shear and turbulence. While back trajectories are more accurate aloft, there are no systematic measurements of air quality above the surface so that verification of model forecasts above the surface is not possible.

The depth of the mixed layer can have a profound effect on pollutant concentrations - particularly wintertime $PM_{2.5}$. Most forecast models provide some measure of the depth of the boundary layer. An example is provided in Figure 8. Determination of boundary layer height is made difficult, however, by the lack of a standard approach for defining its extent (Seibert et al., 2000). Even within the current set of numerical models, there can be systematic differences in retrieved PBL height. Assuming the use of a consistent and accurate boundary layer depth algorithm, an image from the time of maximum boundary layer height (1800-2100 UTC) will be of great usefulness. However, it is also true that the temporal evolution of the boundary layer is often more important than the maximum height reached in the afternoon hours. For example, $PM_{2.5}$ concentrations rise quickly in the morning rush hour. If the surface based inversion persists well into the afternoon hours, averaged $PM_{2.5}$ concentrations will be quite high even though concentrations may decrease briefly during the time of maximum mixing depth. A time series of mixing depth will be useful for diagnosing temporal inversion strength. A clickable map with local potential temperature profiles is useful (Figure 9) although more sophisticated algorithms can be utilized (Table 1).

Combining mixing depth and wind speed information, usually termed a ventilation index, is a frequently used method for ascertaining the extent of stagnation and trapping of pollutants. For PM2.5 forecasts, ventilation index information is often of primary importance to the forecast. The ventilations parameter is usually a simple product of wind speed and mixing depth (m^2s^{-1}). The standard ventilation index is limited by its sensitivity to variations in boundary layer depth. An alternative, developed for use in the Puget Sound, uses the Brunt-Vaisala frequency summed over the lowest layers and over time. (Figure 10).

Forecasts of moisture content are critical for air quality forecasting. To the extent that moisture levels are sufficient to form clouds, it can affect photochemical production of pollutants. Increases in low-level moisture can accelerate gas to particle conversions, e.g., SO_2 conversion to sulfate, and increase $PM_{2.5}$ concentrations. Cloud cover forecasts require additional refinement for use in air quality forecasts. Experience with O_3 forecasting has shown that thin cirrus and shallow cumulus typically have limited effects on concentrations. Optically thick clouds, e.g. stratiform clouds, or clouds that reflect deep vertical mixing, e.g., towering cumulus, can modulate pollutant concentrations. Any measure of cloud cover must therefore take into account cloud depth and optical thickness. This can be accomplished by showing cloud cover at several layers (Figure 11), downward UV flux at the surface (Figure 12) or a time series of RH cross-sections (Figure 13). Low-level moisture and advection, critical for $PM_{2.5}$ forecasts, can also be displayed in a number of ways including wind flags and 1000-850 mb layer mean RH (Figure 14).

4. PROPOSED SUITE OF PRODUCTS

Proposed suites of four panel charts are given for O_3 (Figure 15) and $PM_{2.5}$ (Figure 16). A set of time series panels is provided in Figure 17 and a table of possible additional images is given (Table 1). The four panel charts represent a sub-set of key images that allow air quality forecasters to quickly orient themselves to the critical forecast questions for that day. The additional images in Table 1 would then be of use for more detailed analysis.

5. DISCUSSION AND CONCLUSION

Air quality forecasting, by the nature of the phenomena, requires a specific set of forecast images of both the chemical-transport model and its underlying meteorological model. The critical forecast issues for air quality typically include, the forecast of the pollutant of interest, persistence of the pollutant, magnitude of expected photochemical activity (cloud cover), boundary layer depth, moisture gradients in the boundary layer, transport processes above the nocturnal boundary and near-surface winds.

A proposed suite of forecast images, displayed as a standard four panel chart, will address these issues by providing forecasters with information on the key processes noted above. In addition to providing a check on the forecast model consistency, for example, O_3 fields should reflect cloud cover effects, these panels will allow forecasters to effectively add expert analysis to the forecast. This is particularly valuable in the initial years of numerical model deployment. The forecasting of air quality parameters is a very difficult prospect due the large uncertainty of critical model inputs (e.g., emissions, radiative effects) and the scale of variations (typically meso-γ scale) observed in the forecasted parameters. Model performance is not expected to be as accurate as current meteorological models and is likely to be more on the magnitude of quantitative precipitation forecasts (QPF). Experienced forecasters, however, will be able to deduce the effect on observed concentrations of certain meteorological factors. For example, re-circulation along the land-sea boundary near large emission sources can result in high concentrations affecting certain key monitors. Knowing that the forecast models predict the circulation will occur, forecasters can accurately "correct" the model pollutant forecast for that location.

Eventually, air quality forecast models will achieve a consistency and reliability so that accurate model output statistics (MOS) forecasts can be derived. These products, coupled with forecast images such as those proposed in this paper, will be a major step toward increases in forecast accuracy. Even without a long term "frozen" model, effective MOS products can be developed (Wilson and Vallee, 2003)

ACKNOWLEDGEMENTS

The authors acknowledge the Delaware Valley Regional Planning Commission and Mr. Ron Roggenburk and Mr. Micheal Boyer for their continued support of research in the area of air quality forecasting as well as the Air and Radiation Management Administration of the Maryland Department of the Environment and Mr. Tad Aburn. This paper was developed, in part, at a work shop for the USWRP and many member of our sub-group made useful comments including Jeff McQueen and Paula Davidson from NOAA, and Nelson Seaman from Penn State.

REFERENCES

Dickerson, R. R., B. G. Doddridge, and K. Rhoads, 1995: Large scale pollution of the atmosphere over the remote North Atlantic: Evidence from Bermuda. *J. Geophys. Res*., **100**, 8945-8952.

Draxler, R.R. and Rolph, G.D., 2003. HYSPLIT (HYbrid Single-Particle Lagrangian Integrated Trajectory) Model access via NOAA ARL READY Website (http://www.arl.noaa.gov/ready/hysplit4.html). NOAA Air Resources Laboratory, Silver Spring, MD.

Hamill, T. M., 2003: Evaluating forecasters' rules of thumb: A study of *d*(prog)/dt), *Weather and Forecasting*, **18**, 933-937.

Knapp, K. G., B. B. Balsley, M. L. Jensen, H. P. Hanson, and J. W. Birks, 1998: Observations of the transport of polluted air masses from the northeastern United States to Cape Sable Island, Nova Scotia, Canada, during the 1993 NARE summer intensive. *J. Geophys. Res*., **103**, 13399-13411.

Mass, C., et al., 2003: Regional environmental prediction over the Pacific Northwest, *Bull. Amer. Met. Soc.*, **84**, 1353-1366.

McHenry, J. N., W. F. Ryan, N. L. Seaman, C. J. Coats, Jr., J. Pudykeiwicz, S. Arunachalam, and J. M. Vukovich, 2003: A real-time Eulerian photochemical model forecast system: Overview and initial ozone forecast performance in the NE US Corridor, accepted for publication, *Bull. Amer. Met. Soc.*

McHenry, J. N. et al., 2000: The NCSC-PSU numerical air quality prediction project: Initial evaluation, status, and prospects, *Symposium on Atmospheric Chemistry in the 21st Century*, American Meteorology Society, Boston, 95-102.

Rolph, G.D., 2003. Real-time Environmental Applications and Display sYstem (READY) Website (http://www.arl.noaa.gov/ready/hysplit4.html). NOAA Air Resources Laboratory, Silver Spring, MD.

Ryan, W. F., B. G. Doddridge, R. R. Dickerson, R. M. Morales, and K. A. Hallock, 1998: Pollutant transport during a regional O_3 episode in the mid-Atlantic states, *J. Air & Waste Manage. Assoc*., **48**, 786-797.

Ryan, W. F., C. A. Piety, and E. D. Luebehusen, 2000: Air quality forecasts in the mid-Atlantic region: Current practice and benchmark skill, *Wea. Forecasting*, **15**, 46-60.

Seibert, P., F. Beyrich, S.-E. Gryning, S. Joffre, A. Rasmussen and P. Tercier, 2000: Review and intercomparison of operational methods for the determination of the mixing height, *Atmos. Environ*., **34**, 1001-1027.

Stein, A.F., D. Lamb, R.R. Draxler, Incorporation of detailed chemistry into a three-dimensional Lagrangian-Eulerian hybrid model: application to regional tropospheric ozone, 2000: Atmos. Environ., 34, 4361 - 4372.

Wilson, L. J. and M. Vallee, 2003: The Canadian updateable Model Output Statistics (UMOS): Validation against perfect prog, *Weather Forecasting*, **18**, 288-302.

Table 1. Air quality and meteorological model images useful to operational air quality forecasters.

(a) Model Pollutant Forecasts

Maximum concentrations (time averages vary with pollutant of interest)
Hourly loop of concentrations
Lagged forecasts (12-24 hours) valid at the same time.
Change in pollutant forecast over past model run (current forecast- 24 h prior forecast).
Model performance and bias over short time scale (24-72 h).
Model performance and bias over long time scale (3-14 days).
Concentrations of key precursors (NO_x, SO_2)
Forecasts of pollutant concentrations above the near surface layer, particularly in the “transport” layers above the nocturnal boundary layer.

(b) Persistence Measures

Near real time concentrations (1600 UTC).
Near real time concentrations with back trajectory forecast.
Short term forecast skill (forecast (~ 4 h) – observed concentrations).
Change in observed concentrations of the pollutant over preceding 24-48 hours.

(c) Boundary Layer Depth

Model derived planetary boundary layer height
Ventilation index (a variety of forms possible) coupled with wind flags at predetermined levels
Temperature and wind fields – temperature advection (925 mb, 850 mb)
Change in temperature (ΔT) at selected levels (925 mb, 850 mb)
Vertical profile time series at specific monitors: potential temperature, virtual potential temperature, PBL height.

(d) Moisture
Layer averaged relative humidity: 1000-850 mb, or similar levels.
Advection of relative humidity within boundary layer (e.g., 925 mb) or averaged over a layer.
Vertical profile time series at specific monitors: relative humidity.
Change in relative humidity over 12-24 h intervals at surface and aloft.

(e) Photochemistry
Cloud cover – disaggregated by: height and thickness
Short wave UV flux at the surface

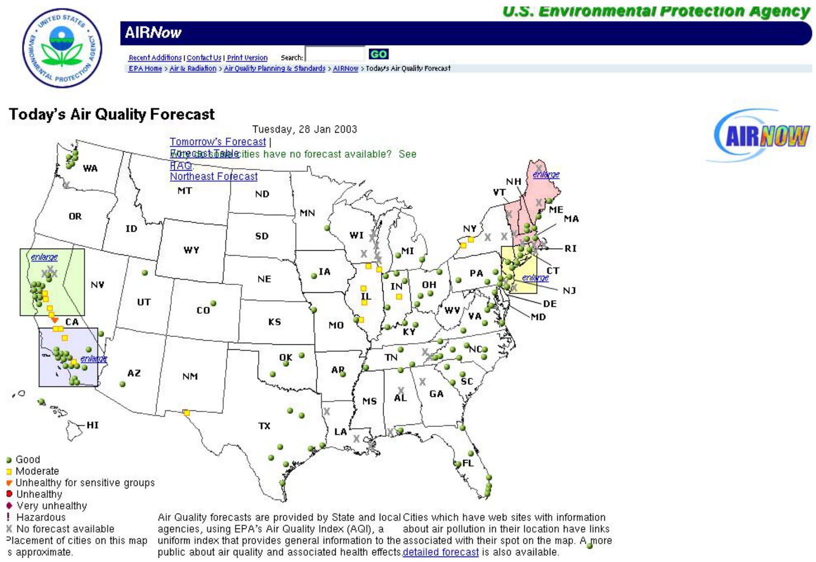

Figure 1. Forecast map from the EPA AIRNow website (http://www.epa.gov/airnow) showing locations that provide routine daily air quality forecasts.

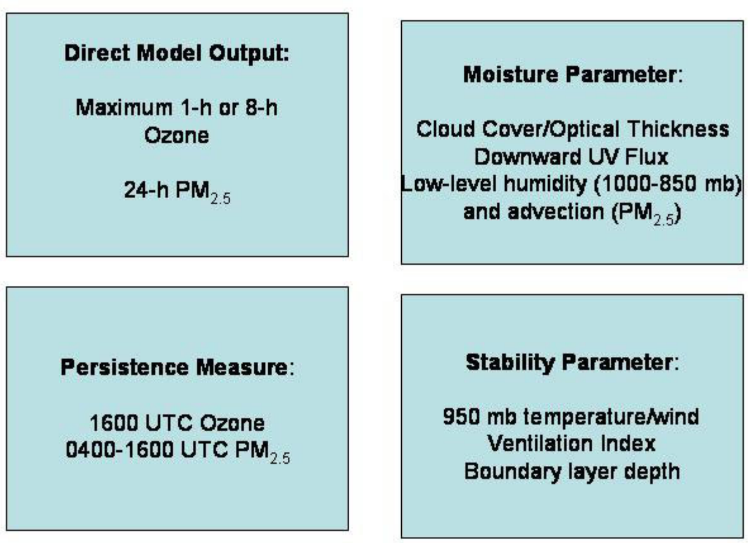

Figure 2. Proposed framework for the air quality four-panel chart.

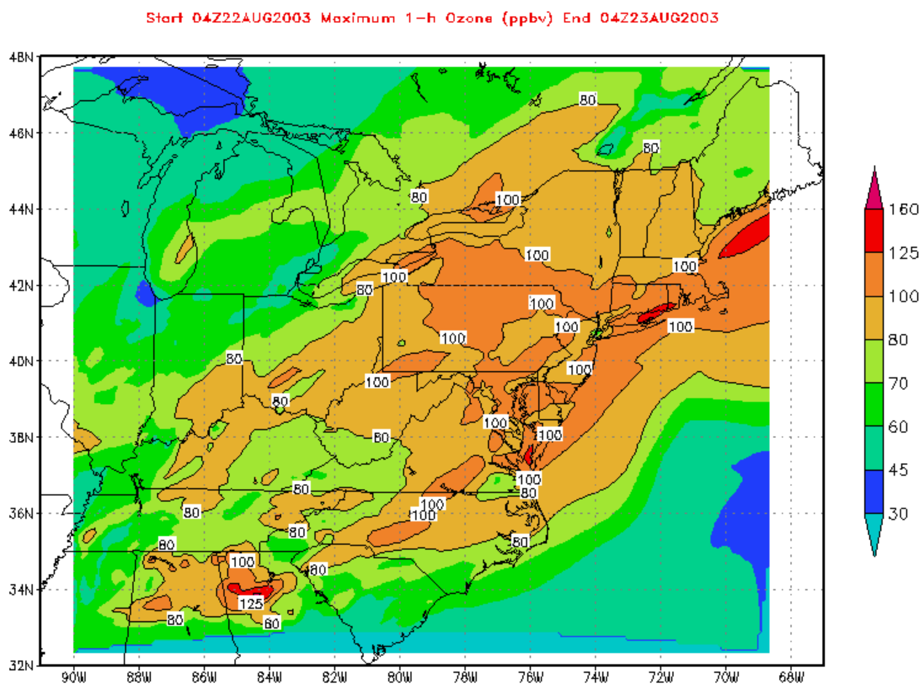

Figure 3. Peak 1-hour O_3 forecast from the NOAA experimental air quality forecast model system for August 22, 2003. Units are parts per billion by volume (ppbv).

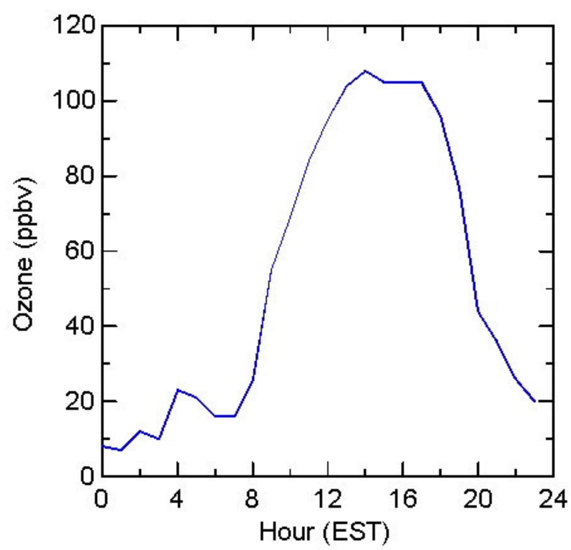

Figure 4. Hourly O_3 concentrations at Fair Hill, Maryland on June 24, 1997.

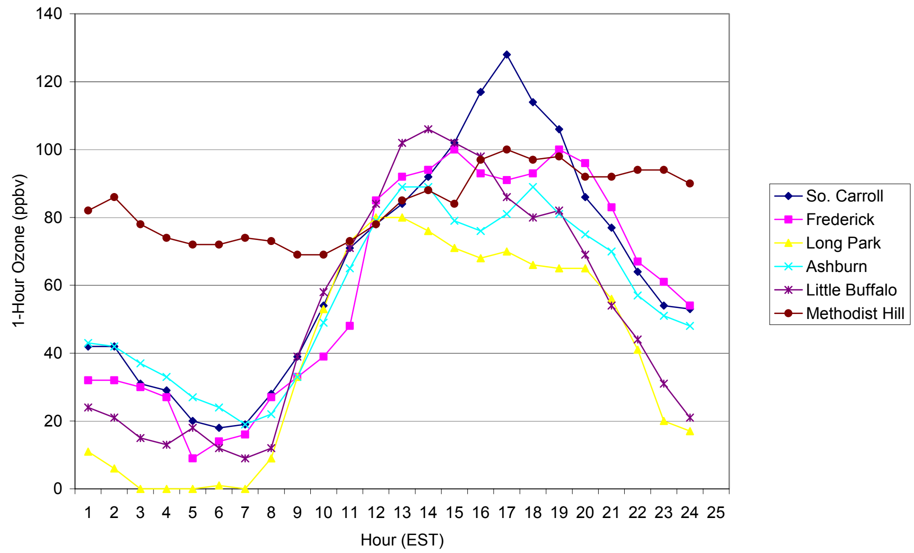

Figure 5. Hourly O_3 concentrations for a series of monitors located west of the I-95 Corridor in the mid-Atlantic for July 17, 1999. The monitors range from west of Washington DC (Ashburn) to central PA (Little Buffalo State Park). The high elevation (~ 740 m) monitor at Methodist Hill gives an indication of regional scale O_3 concentrations above the nocturnal boundary layer.

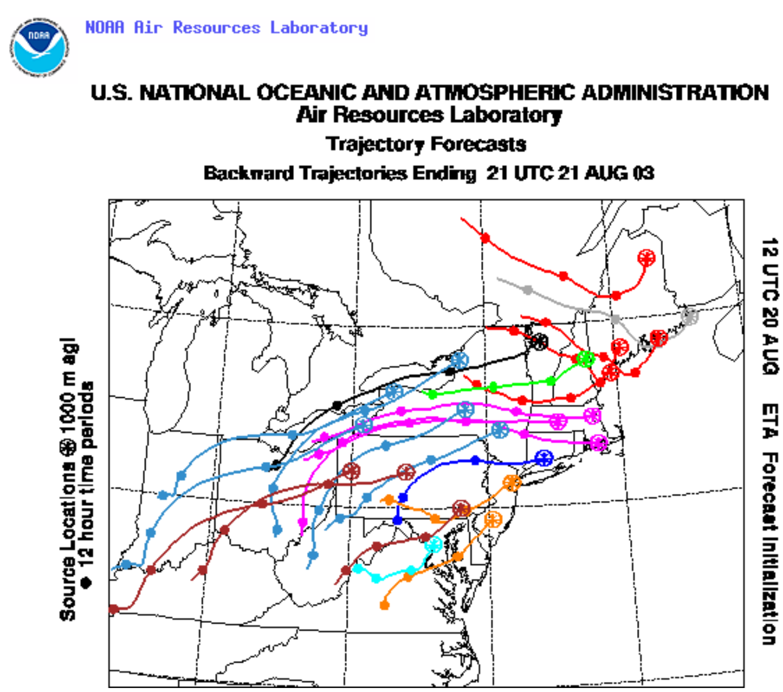

Figure 6. Back trajectories from the NOAA ARL HYSPLIT model for August 21, 2003. The 36-hour trajectories terminate at 2100 UTC at 1000 m above ground level. (See, http://www.arl.noaa.gov/ready/hysplit4.html)

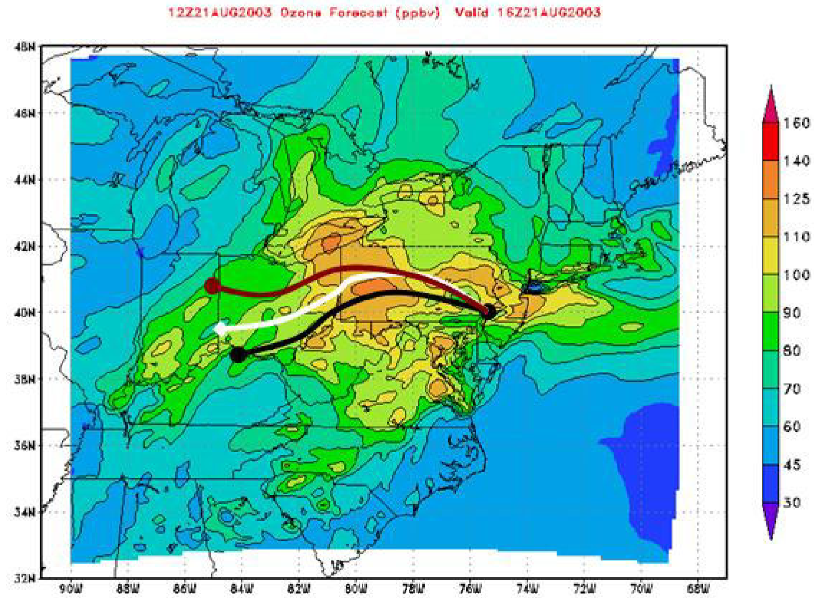

Figure 7. Mockup of observed O_3 data and 24-hour forecast back trajectories. The O_3 data is actually the 4-hour forecast O_3 from the NOAA air quality forecast model for 1600 UTC August 21, 2003 and the back trajectories are simulated from HYSPLIT model results using Eta analysis data (EDAS) for 500 m (black line), 1000 m (white line) and 1500 m (red line) above ground level terminating at 1200 UTC on August 22, 2003.

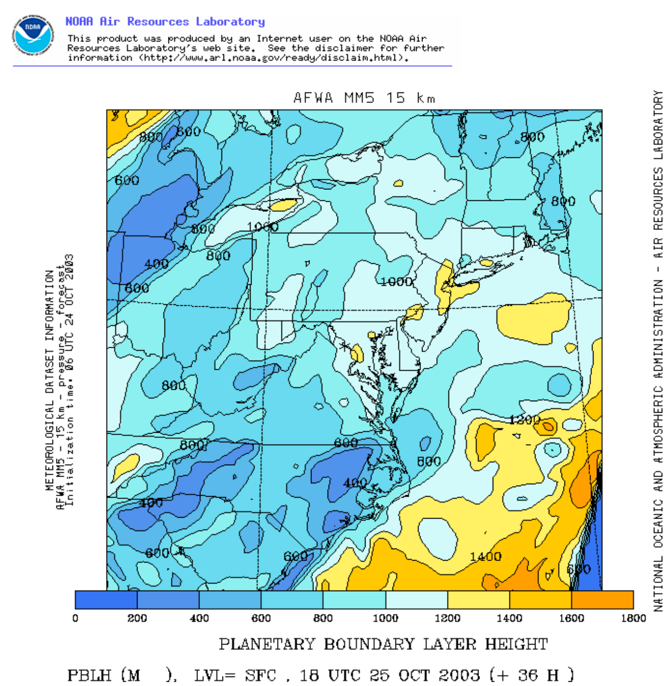

Figure 8. Forecast planetary boundary layer height from the Air Force MM5 model (AFWA) for October 25, 2003. Figure courtesy of NOAA ARL (http://www.arl.noaa.gov/ready/cmet.html).

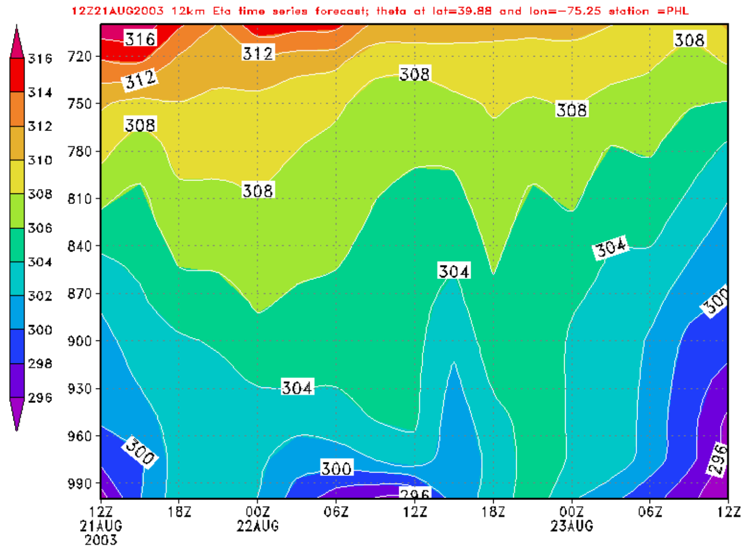

Figure 9. Time series of potential temperature (θ) for Philadelphia from the Eta-12 forecast initialized at 1200 UTC on August 21, 2003 (height is given in millibars).

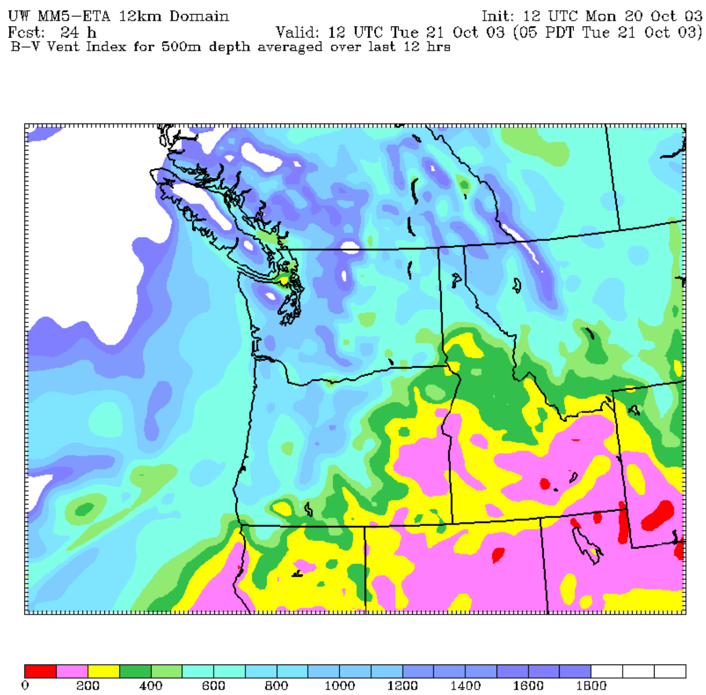

Figure 10. Ventilation index determined from a layer average Brunt-Vaisala frequency for 1200 UTC, October 21, 2003. Figure courtesy of the Northwest Regional Modeling Consortium (http://www.atmos.washington.edu/mm5rt/).

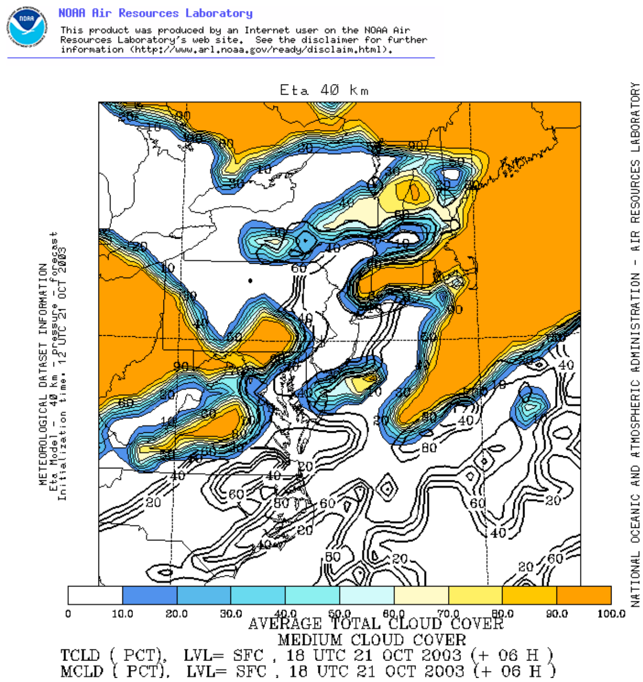

Figure 11. Cloud cover forecast from the NCEP Eta model for 1800 UTC October 21, 2003. Total cloud cover (in percent) is given by black and white contours and mid-level clouds (642-350 mb) are given by color contours. This figure courtesy of NOAA ARL (http://www.arl.noaa.gov/ready/cmet.html).

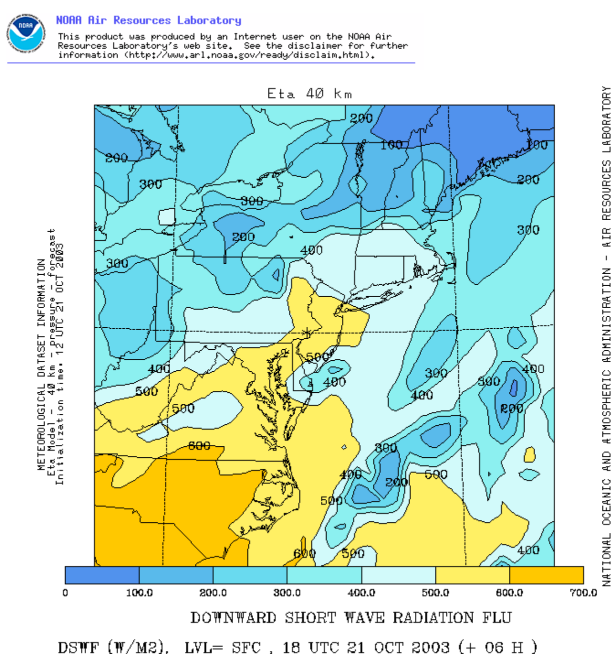

Figure 12. Forecast of downward short wave radiation flux (units of W/m^2) at the surface from the NCEP Eta model for 1800 UTC October 21, 2003. Compare these results with the cloud cover predictions in Figure 11.

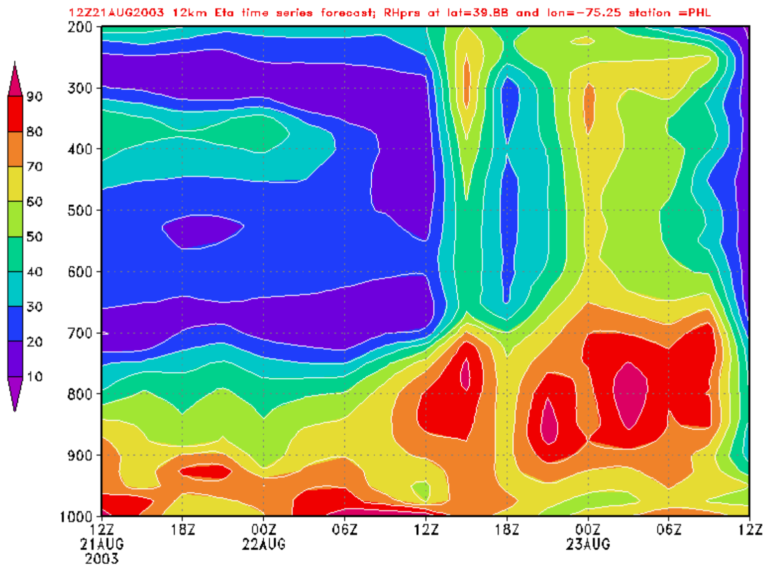

Figure 13. Vertical time series (height is given in millibars) of relative humidity from the NCEP Eta-12 model initialized at 1200 UTC on August 21, 2003.

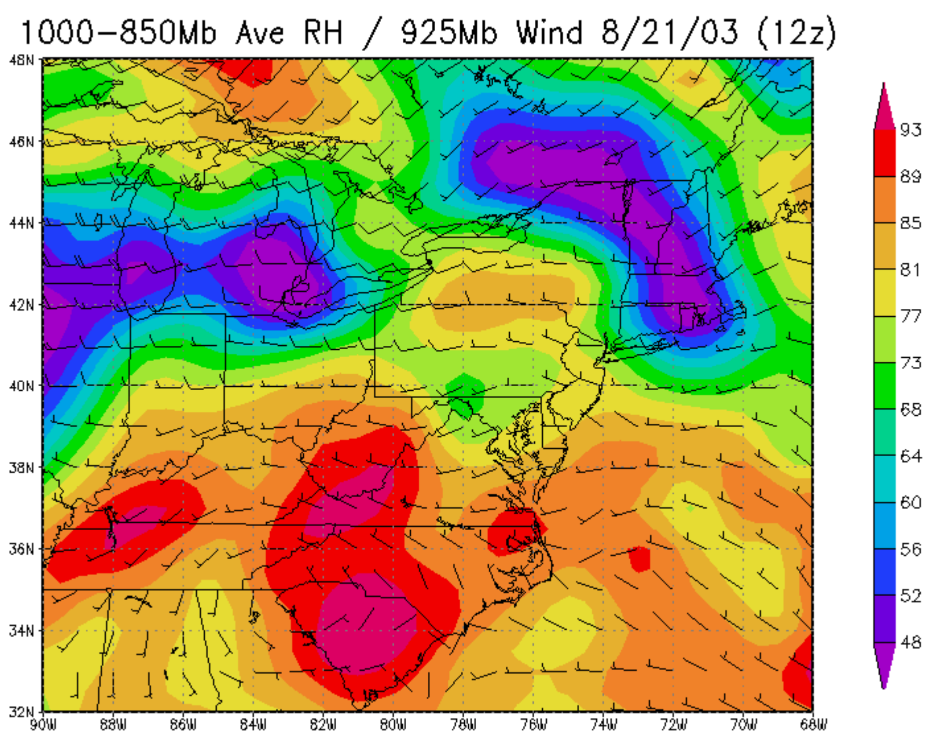

Figure 14. Layer average (1000-850 mb) relative humidity from the NCEP RUC2 analysis for 1200 UTC on August 21, 2003. Relative humidity (in percent) is given by the color contours, with wind barbs (full barbs = 10 ms^{-1}) overlaid.

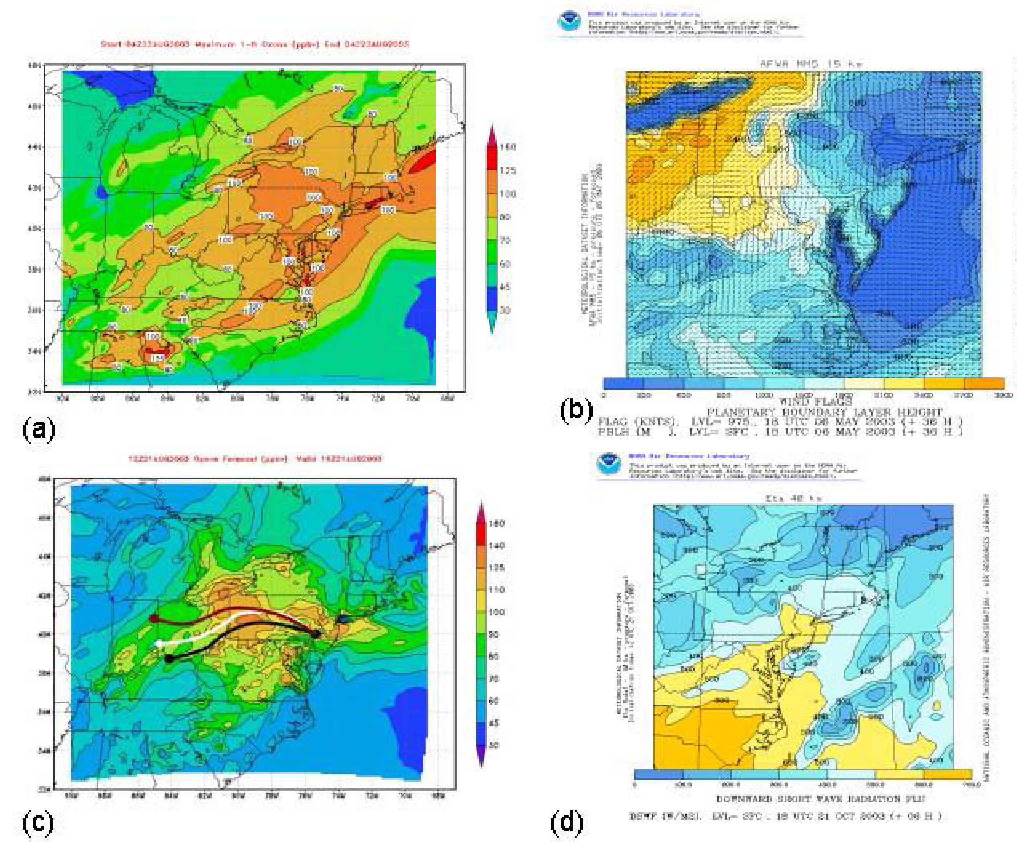

Figure 15. Proposed four panel air quality forecast chart for O_3 forecasting. (a) Maximum 1-hour O_3 concentrations (the panel is from the NOAA experimental forecast for August 21, 2003); (b) Boundary layer height at 1800 UTC (the panel is from the AFWA MM5 forecast for May 6, 2003); (c) O_3 concentrations for 1600 UTC with three- layer back trajectories overlaid (as in Figure 7); (d) Forecast of downward short wave radiation flux (units of W/m^2) at the surface (the image is from the NCEP Eta model for 1800 UTC October 21, 2003).

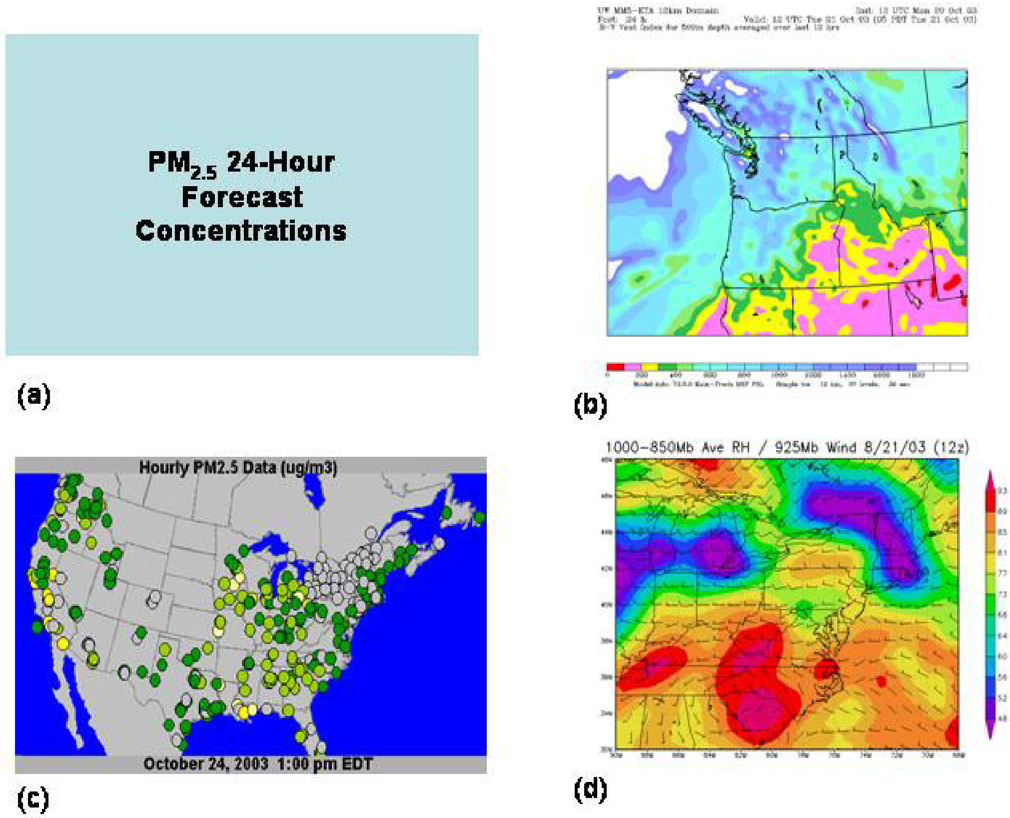

Figure 16. Example of proposed four panel air quality forecast chart for $PM_{2.5}$ forecasting. (a) 24-hour $PM_{2.5}$ concentrations (no image currently available) (b) Ventilation index using Brunt-Vaisala frequency (the panel is from the University of Washington MM5 forecast for October 21, 2003, figure is courtesy of the Northwest Regional Modeling Consortium (http://www.atmos.washington.edu/mm5rt/); (c) $PM_{2.5}$ concentrations for 1700 UTC (the panel contains data from continuous $PM_{2.5}$ monitors and is courtesy of the USEPA and Sonoma Technology. In practice, back trajectories would be overlaid as in Figure 15(c)); (d) Forecast of layer average relative humidity and 925 mb winds (as in Figure 14).

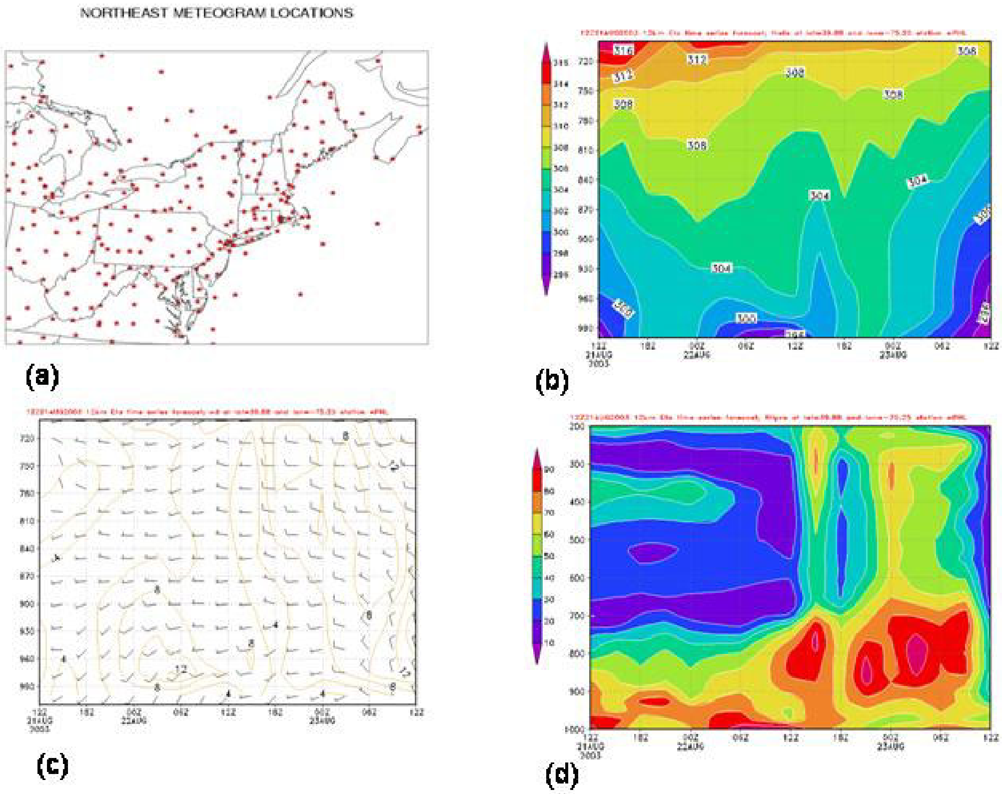

Figure 17. Example of proposed local forecast panels. (a) Clickable map with station locations (Figure courtesy of NCEP EMC: http://wwwt.emc.ncep.noaa.gov/mmb/etameteograms/); (b) Vertical time series (height is given in millibars) of potential temperature (degrees K) for Philadelphia International Airport (PHL) from the NCEP Eta-12 forecast initialized at 1200 UTC on August 21, 2003; (c) as in (b) but for wind (in ms^{-1}); (d) as in (b) but for relative humidity (in percent).